JOURNAL OF GEOPHYSICAL RESEARCH, VOL. 112, E08S07, doi:10.1029/2006JE002853, 2007

Hydration state of the Martian surface as seen by Mars Express OMEGA: 2. H_2O content of the surface

Ralph E. Milliken,[1,2] John F. Mustard,[1] François Poulet,[3] Denis Jouglet,[3] Jean-Pierre Bibring,[3] Brigitte Gondet,[3] and Yves Langevin[3]

Received 1 November 2006; revised 23 February 2007; accepted 3 April 2007; published 29 August 2007.

[1] Visible-near infrared reflectance spectra acquired by the Mars Express Observatoire pour la Minéralogie, l'Eau, les Glaces et l'Activité (OMEGA) spectrometer are used to estimate the absolute water content within the uppermost fraction of the Martian regolith. This upper surface layer represents the boundary between the regolith and atmosphere; thus the amount of water stored in these two reservoirs and at this boundary is expected to vary spatially and temporally with changing equilibrium conditions. We have applied models derived from laboratory experiments relating the strength of the 3 μm hydration feature to absolute water content to OMEGA spectra acquired during the first $\sim$1200 orbits of the Mars Express mission to estimate the H_2O content of the Martian surface. Three methods were used to examine the strength of the 3 μm absorption: integrated band depth, apparent absorbance, and the effective single-particle absorption-thickness (ESPAT) parameter. Integrated band depth and apparent absorbance values are correlated to albedo when derived from reflectance spectra, implying that bright regions are more hydrated than dark regions. The ESPAT parameter, however, relies on single scattering albedo instead of reflectance and is capable of estimating absolute water content within $\pm$1 wt.% H_2O for a wide range of albedo values, compositions, and particle sizes. Applying this model to the OMEGA data reveals that bright and dark regions commonly have similar water contents in equatorial regions and the largest spatial variations in H_2O occur as a function of latitude. Equatorial regions exhibit water contents in the range of $\sim$2–5 wt.%, whereas latitudes higher than $\sim$45°N are characterized by a continuous increase in H_2O with latitude from $\sim$5–15 wt.%. Phyllosilicate and sulfate bearing terrains are more hydrated than average bright and dark regions and their locations are in widely separated areas of Noachian-aged material, suggesting chemical alteration by water-rock interaction may have been spatially extensive in the early history of Mars.

Citation: Milliken, R. E., J. F. Mustard, F. Poulet, D. Jouglet, J.-P. Bibring, B. Gondet, and Y. Langevin (2007), Hydration state of the Martian surface as seen by Mars Express OMEGA: 2. H_2O content of the surface, *J. Geophys. Res.*, *112*, E08S07, doi:10.1029/2006JE002853.

1. Introduction

[2] The role of H_2O in the evolution of Mars is a long-standing problem of planetary science and has been a focal point of the exploration of our neighboring planet. A significant advancement in the understanding of reservoirs other than the polar caps and atmosphere resulted from the detection of large water-ice reservoirs at high latitudes by the Gamma Ray Spectrometer (GRS) on the Mars Odyssey spacecraft [*Feldman et al.*, 2002, 2004b; *Boynton et al.*, 2002; *Mitrofanov et al.*, 2002] and evidence for potentially hydrated phases and sub-aqueous deposition of sediments interpreted from data acquired by the Mars Exploration Rovers (MER) [*Squyres and Knoll*, 2005; *Grotzinger et al.*, 2005; *Squyres et al.*, 2004]. The GRS data are a reasonably direct measurement but are averaged over large spatial scales (100 s of km), whereas MER observations can only be used to infer the role of H_2O over small spatial areas (though spectra acquired by Mini-TES exhibit a distinct H_2O feature near $\sim$6 μm [*Christensen et al.*, 2004]). The Mars Express Observatoire pour la Minéralogie, l'Eau, les Glaces et l'Activité (OMEGA) instrument has the capability to join these spatial and spectral scales through the direct measurement of high spectral (352 channels) and spatial (hundreds of meters to several kilometers) resolution of the uppermost fraction of the Martian surface (depth of up to a few hundred microns).

[1] Department of Geological Sciences, Brown University, Providence, Rhode Island, USA.
[2] Now at Jet Propulsion Laboratory, California Institute of Technology, Pasadena, California, USA.
[3] Institut d'Astrophysique Spatiale (IAS), Orsay Cedex, France.

0148-0227/07/2006JE002853$09.00

[3] The wavelength range of OMEGA (0.38–5.1 μm) [*Bibring et al.*, 2004] includes the fundamental symmetric and asymmetric H_2O stretches centered near ~2.9 μm, the overtone of the H_2O bend at ~3.1 μm (fundamental bend at ~6 μm), and additional overtone and combination vibrational absorptions near ~1.9 and ~1.4 μm. The 1.9 and 3.0 μm features have been observed in OMEGA spectra and were previously used to identify regions containing hydrated sulfates and phyllosilicates [*Bibring et al.*, 2005; *Gendrin et al.*, 2005; *Langevin et al.*, 2005; *Poulet et al.*, 2005], whereas the fundamental H_2O bend near 6 μm has been observed and mapped by other workers using Mars Global Surveyor Thermal Emission Spectrometer (TES) data [*Bandfield and Smith*, 2003; *Ruff*, 2004; *Kuzmin et al.*, 2004]. We have combined laboratory-based models that relate the strength of the 3 μm feature to H_2O content [*Milliken and Mustard*, 2005] with an analysis of the strength of this feature observed in OMEGA data (Figure 1) to provide the first quantitative estimates of the absolute water content of the Martian surface on a global scale. A companion paper by *Jouglet et al.* [2007] presents a detailed description of the calibration and reduction of OMEGA data for the 3 μm region and examines variations in hydration of the Martian surface with season, elevation, albedo, and strength of the 1.9 μm combination overtone hydration band.

[4] Previous studies of VIS-NIR reflectance data have focused primarily on qualitative, not quantitative, comparisons of variations in the strength of the 3 μm band observed for Mars. In agreement with early telescopic observations of the 3 μm feature on Mars [*Sinton*, 1967; *Houck et al.*, 1973], *Bibring et al.* [1989] noted that all spectra acquired by the Phobos-2 Imaging Spectrometer (ISM) instrument exhibited a strong 3 μm band that varied in strength (band depth) between bright and dark regions. Band depth values (see equation (1)) for this 3 μm feature were examined further by *Murchie et al.* [1993] and *Murchie et al.* [2000], who concluded that bright regions commonly have a stronger 3 μm band than dark regions, but regions of intermediate-albedo ("dark red") soils within Lunae Planum exhibit the strongest 3 μm band depths when compared to regions of similar albedo [*Murchie et al.*, 2000]. *Calvin* [1997] used the method of normalized integrated band depth to examine variations in the strength of the 3 μm absorption observed in Mariner 6 Infrared Spectrometer (IRS) data. Unlike the band depth parameter, this method is less dependent on albedo and has the added benefit of accounting for the entire strength and shape of the 3 μm feature, not just the maximum absorption point [*Calvin*, 1997]. Results from the normalized integrated band depth approach suggested high- and low-albedo regions had similar values, at least within the uncertainties of the method and IRS data [*Calvin*, 1997]. However, it has

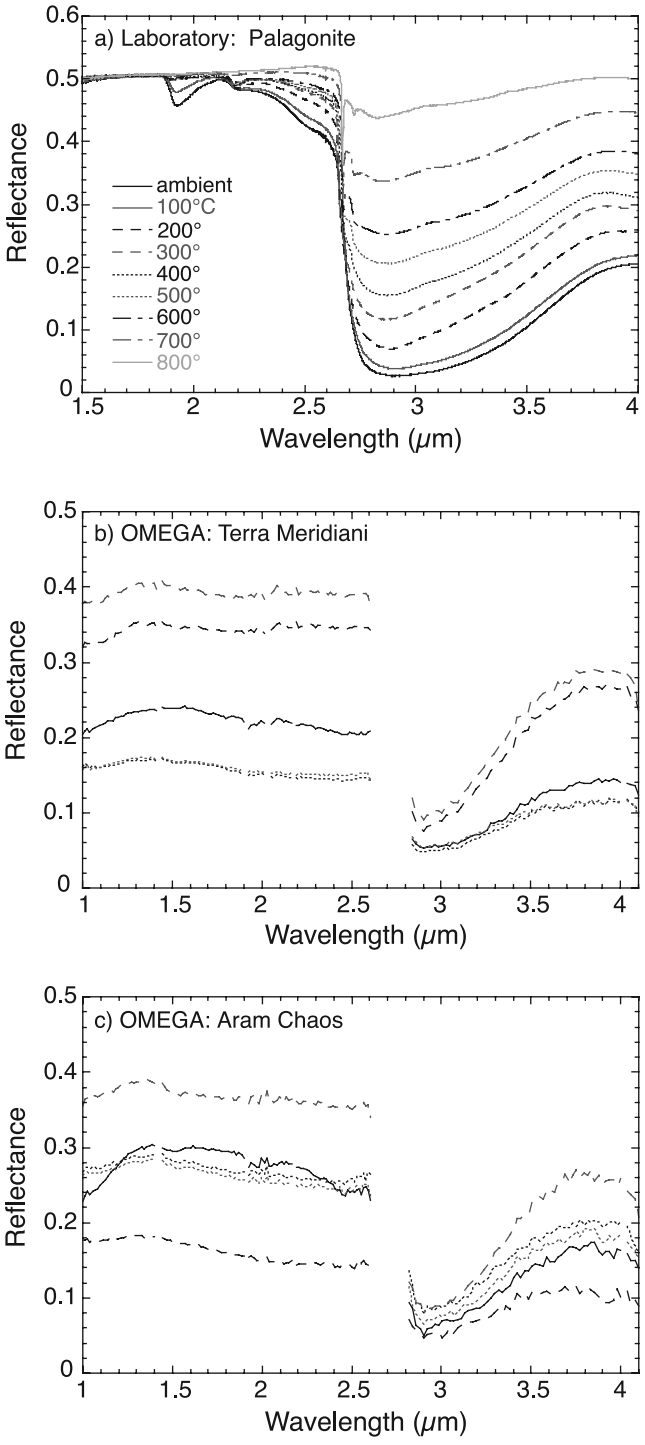

Figure 1. Examples of near-infrared reflectance spectra illustrating variations in the strength and shape of the 3 μm absorption associated with changes in water content. (a) Laboratory spectra (FTIR) of a palagonite heated to different temperatures to decrease water content [*Milliken and Mustard*, 2005]. (b) OMEGA spectra from an observation over Terra Meridiani, a region known to contain sulfates and hematite [*Squyres et al.*, 2004]. The minimum reflectance value within the 3 μm region varies with albedo. (c) OMEGA spectra from an observation over Aram Chaos, also a region that contains sulfates and hematite. The 3 μm band also varies with albedo, and the solid spectrum exhibits a strong 1 μm band and absorptions near ~1.9 and ~2.4 μm, indicative of sulfate [*Gendrin et al.*, 2005]. Strong atmospheric CO_2 bands centered near ~2.7 μm have been masked in Figures 1b and 1c.

been shown by *Milliken and Mustard* [2007a] that both band depth and integrated band depth are strongly correlated to albedo and cannot be used for quantitative estimates of hydration. Given these conflicting results, it is yet undetermined if bright regions on Mars have increased, equivalent, or decreased water contents relative to dark regions.

[5] The only study to attempt a quantitative assessment of water content using the strength of the 3 μm band was that of *Yen et al.* [1998], who compared ISM spectra with laboratory spectra of hydrated phases mixed with anhydrous phases. *Yen et al.* [1998] estimated the water content of the surface to be $\leq$4 wt.% by converting reflectance spectra, R, to apparent absorbance, $-\ln(R)$, to account for the logarithmic compression effects of absorption and scattering. This range includes estimates of the H_2O content of the Martian soil as measured by the Viking landers, which was on the order of $\sim$1–2 wt.% H_2O but may have uncertainties up to a factor of five [*Biemann et al.*, 1977; *Anderson and Tice*, 1979]. The work by *Yen et al.* [1998] provided the foundation for a quantitative estimate of water content using the strength of the 3 μm absorption, but the model had uncertainties in estimated H_2O content of up to $\sim$2 wt.% depending on the composition of the hydrated phase and did not control for particle size or albedo. It has been shown by *Milliken and Mustard* [2005, 2007a] and *Clark* [1983] that parameters such as band depth, integrated band depth, and apparent absorbance (or mean optical path length) will be correlated to albedo when derived from reflectance data, further complicating the comparison of absorption strengths and estimates of water content between high- and low-albedo regions on Mars.

[6] The ISM instrument provided data of high spectral resolution for Mars, but like Mariner IRS data were of relatively low spatial resolution and only covered a small portion of the planet. The Mars Odyssey GRS instrument suite consists of the Gamma Ray Spectrometer, High Energy Neutron Detector (HEND), and the Neutron Spectrometer (NS), where the latter is capable of measuring fast, thermal, and epithermal neutrons and provided the first global estimates of water-equivalent hydrogen (WEH) in the upper $\sim$1 m of the Martian surface [*Feldman et al.*, 2002; *Boynton et al.*, 2002; *Mitrofanov et al.*, 2002]. However, these data are of very low spatial resolution and have a footprint with a diameter of $\sim$600 km [*Feldman et al.*, 2004b]. Nevertheless, analysis of the NS and HEND data has detected the presence of a large reservoir of H^+ possibly buried under several centimeters of a ''dry'' regolith poleward of $\pm$50° latitude and over a vast equatorial region corresponding to Arabia Terra [*Feldman et al.*, 2002; *Boynton et al.*, 2002; *Mitrofanov et al.*, 2002]. The concentration observed for the former reservoir (upwards of 40 wt.% WEH) is higher than would be expected for most hydrated minerals [*Feldman et al.*, 2002] and ice stability models suggest that the H^+ is predominantly in the form of water ice, whereas models of near-surface ice stability preclude this possibility for the latter [*Mellon and Jakosky*, 1995], implying the H^+ is likely present in the form of hydrated minerals such as clays, sulfates, or zeolites [*Fialips et al.*, 2005; *Feldman et al.*, 2004a; *Vaniman et al.*, 2004; *Bish et al.*, 2003].

[7] Converting the Neutron Spectrometer data to accurate estimates of wt.% H_2O or water-equivalent hydrogen (WEH), however, requires some knowledge of the ''abundance of water and its gradient with depth'' [*Feldman et al.*, 2004b]. Recent estimates of WEH by *Feldman et al.* [2004b] were based on a 2-layer model that assumed the upper layer, of unknown thickness, contained 2 wt.% H_2O. This value was then used to find the best fit model to the GRS data, solving for the thickness of the ''dry'' 2 wt.% layer and the WEH abundance of the lower, semi-infinite layer. The input value of 2 wt.% H_2O was the minimum WEH value determined by using a 1-layer model, with no ''dry'' layer, and assumes that at least one area measured by the Neutron Spectrometer corresponds to a water content that is homogeneous with depth and is representative of the water content of the average soil [*Feldman et al.*, 2004b]. However, the actual spatial variation in water content of the uppermost fraction of the surface is essentially unconstrained; therefore a model that assumes the ''dry'' upper surface has a global homogeneous water content (2 wt.%) may be unrealistic.

[8] Reflectance spectra acquired by the OMEGA instrument, however, are representative of this uppermost portion of the regolith and may be used to estimate the true water content of the ''dry'' layer. The goal of this paper is to estimate the water content of the Martian surface, independent of the GRS and Viking measurements, by examining the strength of the 3 μm hydration feature. We have calculated integrated band depth and apparent absorbance for the OMEGA data as a direct comparison to the previous work of *Calvin* [1997] and *Yen et al.* [1998]. We also convert reflectance data to single scattering albedo and calculate the effective single-particle absorption-thickness (ESPAT) parameter [*Hapke*, 1993], for which *Milliken and Mustard* [2005, 2007a] showed hydration estimates to be independent of albedo over a range that includes values typical of the Martian surface. In this paper we compare our estimates of absolute water content to variations in albedo (to determine the relative hydration between bright and dark soils), the H_2O content of the surface as inferred from measurements by the Viking landers, GRS estimates of WEH in the near-surface, and characterize spatial variations in water content on Mars.

2. Methods

[9] Our confidence in being able to detect changes in water content by examining changes in the strength of the 3 μm hydration feature stems from laboratory results that demonstrate a strong correlation between these two properties. As an example, the laboratory spectral dehydration series of palagonite presented in Figure 1a shows that the strength of the 3 μm band decreases as water is removed from the sample, in this case by heating the palagonite to higher temperatures. Laboratory experiments such as these for a variety of hydrated minerals suggest that spatial variations in the 3 μm band on Mars can be linked to variations in absolute water content [*Milliken and Mustard*, 2005]. Similarly, *Jouglet et al.* [2007] have shown that repeat observations of the same target during different seasons may be used to examine changes in surface

hydration related to changes in the local or seasonal abundance of atmospheric water vapor.

[10] As discussed above, previous workers noticed a correlation between the strength of the 3 μm feature and albedo using ISM data [*Murchie et al.*, 2000]. This general trend is also evident in the OMEGA spectra presented in Figures 1b and 1c, though there are also exceptions. The spectra corresponding to bright surfaces in Figure 1b (dashed spectra), for instance, have a higher reflectance at 3 μm than the spectra for low-albedo surfaces (dotted spectra), but the spectrum for an intermediate albedo surface (solid spectrum, Figure 1b) has a 3 μm reflectance nearly identical to that of the low-albedo surface spectra. This suggests that some of the variations in the strength (reflectance value) of the 3 μm band must be related to actual differences in water content and not simply albedo, similar to the differences in the 3 μm band observed for the various hydration states of palagonite in Figure 1a (see *Milliken and Mustard* [2007a] for a detailed analysis of low-albedo hydrated materials). A similar trend is apparent for the black, solid spectrum in Figure 1c, which has similar or slightly higher reflectance values than the dotted spectra for wavelengths shorter than $\sim$2.5 μm but lower reflectance values for wavelengths longer than 2.5 μm (i.e., a stronger 3 μm band). This spectrum also exhibits additional absorptions in the 1–2.5 μm region, suggesting it may represent a different composition from the surrounding terrains. We will utilize these differences in the strength of the 3 μm absorption and their relation to water content in order to quantify the hydration sate of the Martian surface.

2.1. OMEGA Data Processing

[11] The OMEGA observations used for this study have been photometrically corrected for all known instrument responses to convert data from raw DN values to spectral radiance (W/m^2/sr/μm). Radiance values for wavelengths >3 μm contain a non-negligible component of thermally emitted radiance in addition to reflected radiance for a wide range of kinetic surface temperatures [*Jouglet et al.*, 2007]. The thermally emitted radiance has been removed from the observed radiance using the method of *Jouglet et al.* [2007]. This method derives the surface temperature by first estimating the emissivity (= 1 − R) at 5 μm using the observed reflectance at $\sim$2.5 μm, which is approximated by dividing the observed radiance by the solar radiance and the cosine of the incidence angle. A linear relationship between reflectance values at these two wavelengths is then defined by the average bright and dark region spectra of Mars as determined by *Erard and Calvin* [1997]. We correct the data for a nominal 1-pixel spatial offset (along ground track of the spacecraft) that exists between the two short-wavelength infrared (SWIR) detectors that span the $\sim$1–5 μm region prior to the thermal correction.

[12] Our band parameters, which are discussed in detail below, assume a straight-line continuum fit over the 3 μm absorption as defined by the maximum reflectance near $\sim$2.5 μm. This method is based on laboratory observations that the $\sim$4 μm reflectance increases to a value equivalent to that at $\sim$2.5 μm as hydrated phases dehydrate [*Milliken and Mustard*, 2007a]. We interpret the negative slope between the short and long wavelength sides of the 3 μm band to result from the presence of H_2O and find that our predictions of water content have smaller residuals when assuming a straight-line continuum [*Milliken and Mustard*, 2007a]. This method of continuum removal has the additional advantage that it does not depend on the reflectance value at $\sim$4 μm, which has a larger proportion of thermally emitted radiance than at $\sim$3 μm and is thus less dependent on an accurate thermal correction.

[13] The thermally corrected data are divided by a scaled atmospheric gas absorption spectrum following the method of *Mustard et al.* [2005], the incident solar radiance at Mars distance, and the cosine of the incidence angle to retrieve apparent Lambert albedo. The data have not been corrected for the presence of aerosols or water-ice clouds. We grid the band parameter values at 32 pixels per degree (approximately 2 km × 2 km at the equator) and place higher spatial resolution observations on top of lower spatial resolution observations. The results presented here range in spatial resolution from <1 km to $\sim$3 km per pixel; therefore some regions are oversampled, whereas others are undersampled. Band parameter values are not averaged because the spectra have not been corrected for the presence of aerosols or water ice clouds, which may introduce changes in reflectance levels, particularly at shorter wavelengths. We do not include data acquired at incidence angles >60° or emergence angles >20° in order to minimize viewing geometry and corresponding aerosol effects on our results. Spectra are filtered for these effects prior to placing the data in the grid, thus minimizing artifacts in the final product that are not representative of surface hydration. We filter the data for surface frost and water-ice clouds by eliminating spectra that have a band depth value at 1.5 μm (overtone absorption in H_2O ice) greater than 0.5%. This is similar to the method used by *Jouglet et al.* [2007], who also examine potential effects and uncertainties that might arise from the presence of small ice patches that lack a 1.5 μm band and only affect the 3 μm region. The majority of data presented here were acquired during the first $\sim$500 orbits of the mission, corresponding to early northern spring/northern summer and a time when the atmosphere appeared to be relatively clear and free of clouds.

[14] This study only examines data acquired during orbits for which the response of the OMEGA instrument is at the nominal calibration level (orbits 18–518, 905–1206) and the current photometric corrections yield reliable radiance values in the 3 μm region [*Jouglet et al.*, 2007]. Observations in the "nominal" calibration state correspond to orbits for which observed values of the onboard calibration lamp are close to $\sim$1500 DN for the $\sim$2.5–5.1 μm region, whereas observations with values significantly below this level are in a "low" state [*Jouglet et al.*, 2007]. The exact cause of this "low" state and how to correct radiance values accordingly has not yet been determined. Characterizing this phenomenon is an ongoing process and thus we will only consider data in the "nominal" state, similar to *Jouglet et al.* [2007]. This excludes a large portion of the data set, but it is necessary for an accurate quantitative analysis of the hydration feature. An OMEGA albedo map (reflectance value at 2.5 μm) showing the spatial coverage of the data used for this study is presented in Figure 2. The nonuniform shape within and between observations is a result of the elliptical orbit of the Mars Express satellite and the

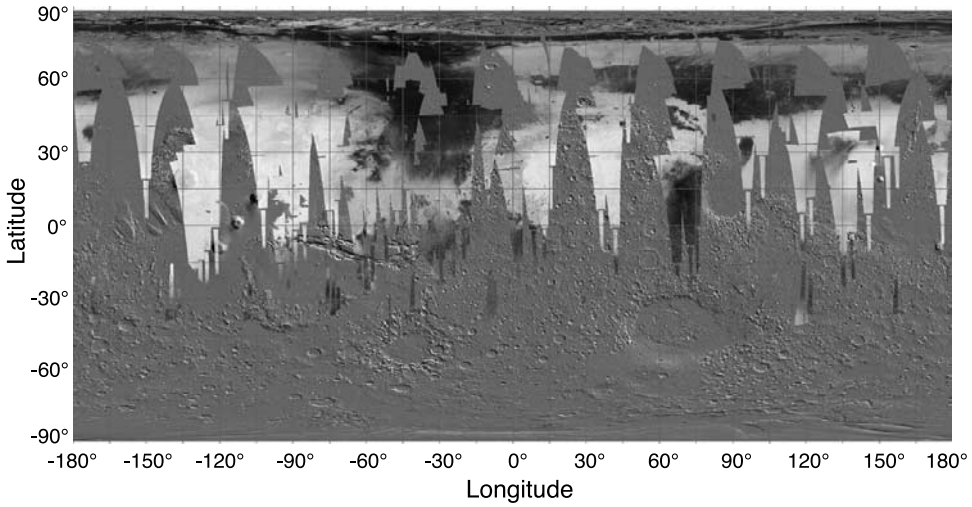

Figure 2. Map of apparent Lambert albedo at ~2.5 μm for OMEGA observations used in this study. These observations correspond to orbits for which the response of the OMEGA instrument was at the nominal calibration state (primarily orbits <518). The background is a hill shade image of MOLA topography.

various operating modes of OMEGA (16, 32, 64, and 128 pixel-width modes) [*Bibring et al.*, 2004].

2.2. Estimating Water Content

2.2.1. Integrated Band Depth

[15] The band depth parameter is commonly defined as the minimum reflectance value within an absorption relative to the continuum value at that same wavelength [*Clark and Roush*, 1984], such that

$$BD_\lambda = 1 - \frac{R_{b,\lambda}}{R_{c,\lambda}} \tag{1}$$

where R_b is the reflectance at the band minimum and R_c is the reflectance of the continuum fit. A strong, saturated absorption ($R_b = 0$) will have a BD value of 1 and a region with no absorption ($R_b = R_c$) will have a band depth of 0. We follow the method of *Milliken and Mustard* [2005] and define that integrated band depth for the 3 μm absorption as

$$IBD_{3\,\mu m} = \left[\int_{\lambda=\lambda_{\min}=2.81\,\mu m}^{\lambda=\lambda_{\max}=3.9\,\mu m} 1 - \frac{R_b(\lambda)}{R_c(\lambda)} \right] \Big/ \cdot \left[(R_c(2.81)) \cdot (\lambda_{\max} - \lambda_{\min}) \right] \tag{2}$$

The denominator in (2) normalizes the IBD by the area encompassed by the continuum fit and the wavelength range of the integration, forcing IBD values to range between 0 and 1. We assume a straight-line continuum; therefore $R_c(3.9\ \mu m) = R_c(2.81\ \mu m)$. The width of the 3 μm absorption is quite consistent for most of the Martian surface as observed in OMEGA spectra; thus we choose a constant maximum wavelength value of 3.9 μm for the integration and normalization in equation (2). The integrand in (2) is evaluated for OMEGA spectra by summing the product of the wavelength difference and average reflectance value for pairs of consecutive channels between 2.81–3.9 μm.

2.2.2. Apparent Absorbance

[16] As discussed earlier, converting reflectance values to apparent absorbance [*Kortum*, 1969] or mean optical path length (apparent absorbance divided by the absorption coefficient) [*Clark and Roush*, 1984] is a simple approach for linearizing the exponential effects of absorption processes [*Yen et al.*, 1998]. In order to account for differences in albedo between bright and dark regions on Mars, which can affect the absolute reflectance values for the 3 μm band, we determine the apparent absorbance relative to the continuum, such that

$$AppAbs_\lambda = -\ln\left(\frac{R_{b,\lambda}}{R_{c,\lambda}}\right) \tag{3}$$

Again, the continuum is as a straight-line defined by the maximum reflectance value near ~2.5 μm. The value of R_b for the OMEGA data (and most H_2O-bearing materials) is commonly taken at ~2.9 μm. We calculate the value of R_b for OMEGA spectra by averaging values from the minimum and adjacent short and long wavelength channels.

2.2.3. ESPAT Parameter

[17] The final parameter that we consider for this study is the effective single-particle absorption-thickness (ESPAT) as defined by *Hapke* [1993]. This parameter is dependent on the extinction, absorption, and scattering efficiencies, Q_E, Q_A, and Q_s, respectively, and is defined as

$$ESPAT_\lambda = \frac{Q_{E,\lambda} - Q_{S,\lambda}}{Q_{S,\lambda}} = \frac{1 - w_\lambda}{w_\lambda} \tag{4}$$

in which w is the single scattering albedo. We convert OMEGA apparent reflectance data to single scattering albedo using the method of *Hapke* [1993], where the bi-directional reflectance distribution factor (BRDF) is defined as

$$BRDF = \frac{r}{\mu_o} \tag{5}$$

and can be related to w by

$$R_{apparent} \approx BRDF(i,e,g) = \frac{w}{4}\frac{1}{\mu_o + \mu} \cdot \{[1 + B(g)]p(g) + H(\mu_o)H(\mu) - 1\} \quad (6)$$

[18] Here, r is the bi-directional reflectance, i is the incidence angle, e is the emergence angle, μ_o is the cosine of the incidence angle, μ is the cosine of the emergence angle, and g is the phase angle. The relationship between the BRDF and w presented by *Hapke* [1993] includes an additional factor of π in the denominator on the right-hand side of equation (6). This is because *Hapke* [1993] defines the bi-directional reflectance, r, as the radiance observed at the detector, I, divided by the solar irradiance, J, which are related by

$$r = \frac{I_{detector}}{J_{solar}} = \frac{I_{detector}}{I_{solar} \cdot \pi} \quad (7)$$

The solar spectrum used with the OMEGA data, however, is in units of radiance and has already accounted for the factor of π (i.e., the OMEGA values of r used in (5) are radiance divided by radiance, not radiance divided by irradiance); therefore we use the formula presented in (6) for the BRDF and not that presented by *Hapke* [1993].

[19] The H function in equation (6) is approximated by *Hapke* [1993] as

$$H(x) \approx \frac{1 + 2x}{1 + 2x\sqrt{1 - w}} \quad (8)$$

[20] We assume the surface of Mars is characterized by isotropic scattering, such that $p(g) = 1$, and that the opposition effect is negligible, such that $B(g) = 0$. Therefore only three parameters are required to invert (6) and solve for the single scattering albedo: i, e, and R_{app}, all of which are known. We recognize that the surface of Mars may in fact be slightly backscattering and not isotropic, such that $B(g)$ is negative, but exact values for this parameter are currently unknown on local or global scales. However, isotropic scattering has been shown to be an adequate assumption for small particles in contact, as is the case for a planetary regolith [*Mustard and Pieters*, 1989; *Piatek et al.*, 2004]. The right-hand side of equation (4) assumes that the extinction efficiency is one; therefore we remove a straight-line continuum from the w spectra over the 3 μm region such that the ESPAT parameter is equal to 0 when there is no water absorption.

[21] Similar to the apparent absorbance, the value of w at is taken to be the average of the three minimum values in the 3 μm region, commonly near $\sim$2.9 μm. We note that the value of the single scattering albedo (w) at any given wavelength will depend on both the absorption coefficient (α) and the path length (d) of the material. Furthermore, the path length can be directly related to the particle size of the material [*Hapke*, 1993]; thus the value of $H(x)$ in equation (8) is also dependent on particle size. The effects of particle size on our hydration model are discussed further below and by *Milliken and Mustard* [2007b]. We also note that in this work when comparing reflectance spectra from one region to another we are assuming the surface is smooth on scales larger than the particle size. The effects of shadowing and large-scale roughness variations are assumed to be second order effects since we are integrating over large areas (several kilometers per pixel) and examining data acquired at a variety of incidence and emergence angles. Future work will focus on quantifying the effects of particle size, shadowing, and surface roughness on the hydration model.

3. Results

3.1. Integrated Band Depth and Apparent Absorbance

[22] Maps of the integrated band depth and apparent absorbance values derived using the OMEGA data are compared to albedo values at $\sim$2.5 μm in Figures 3a–3c. Both of these parameters exhibit a correlation to albedo; bright areas such as Arabia Terra and the Tharsis region have higher parameter values compared to low-albedo regions such as Syrtis Major and Acidalia. This albedo-dependence is stronger for the apparent absorbance than the IBD parameter, as evident from the values for the Acidalia region (between $\sim$0–60°W, 30–60°N). If these parameter values are directly related to the hydration state of the surface (amount of H_2O), then the IBD parameter suggests this region may be increased in hydration relative to areas of similar albedo, whereas the apparent absorbance suggests it is not significantly different from other low-albedo regions (Figures 3b and 3c). Both of these parameters suggest a possible increase in hydration with latitude poleward of $\sim$60°N, corresponding to a region of increased water-equivalent hydrogen as seen by the Neutron Spectrometer on Mars Odyssey [*Feldman et al.*, 2004b]. A similar trend was initially observed by *Pimentel et al.* [1974] using Mariner 6 and 7 IRS data. That work used reflectance ratios at 2.2, 2.9, and 3.1 μm to qualitatively evaluate spatial variations in condensed phases of H_2O (either in minerals or as water ice), showing an increase in the amount of condensed H_2O with increasing latitude in the southern hemisphere.

[23] It is impractical to estimate exact values of weight percent H_2O using either of these parameters, however, since laboratory data show that such estimates are dependent on both albedo and composition [*Milliken and Mustard*, 2005, 2007a]. The albedo is known in this case, but the composition of the surface and the hydrated phases are too poorly constrained on a global scale to provide a reasonable estimate of the relationship between the IBD parameter and wt.% H_2O or apparent absorbance and H_2O. The data of *Yen et al.* [1998] show an exponential relationship between apparent absorbance and water content that could be used to estimate the absolute water content of the surface, but this method has an uncertainty of $\sim$2 wt.% H_2O for the hydrated phases examined in that study. Furthermore, the measurements of *Yen et al.* [1998] did not control for albedo or particle size variations. Given the albedo dependence and uncertainties in water content derived from apparent absorbance, we will not attempt to estimate absolute H_2O content using this parameter here.

[24] We emphasize that the integrated band depth and apparent absorbance values are correlated to albedo, giving the impression that bright regions may be more hydrated than dark regions, and increase north of $\sim$60° latitude.

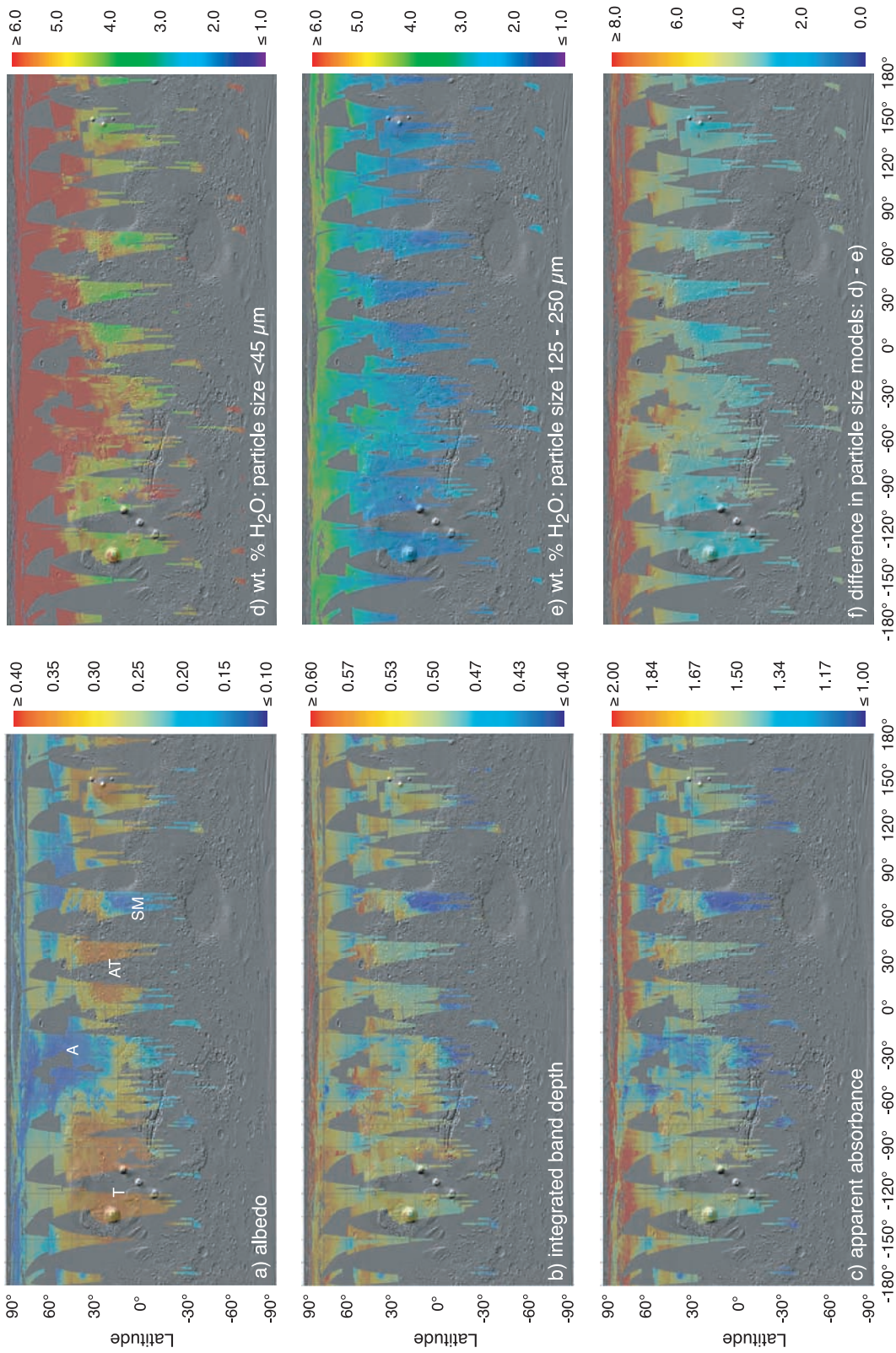

Figure 3. Maps of (a) albedo at ~2.5 μm, (b) integrated band depth, (c) apparent absorbance, (d) water content assuming particle size <45 μm, (e) water content assuming particle size of 125–250 μm, and (f) the difference, in wt.% H_2O, between Figures 3d and 3e. Values for Figures 3b and 3c exhibit a positive correlation to albedo, though both of these parameters also suggest an increase in hydration for latitudes poleward of ~60°N. All values of wt.% H_2O are derived from the ESPAT parameter. Though the differences in absolute values presented in Figure 3f are large, the relative relationships in hydration between regions are similar for each model. A, Acidalia Planitia; AT, Arabia Terra; SM, Syrtis Major; T, Tharsis.

Table 1. Slopes of Best Fit Lines for the Various Relationships Between Observed ESPAT Values at 2.9 μm and Predicted Values of wt.% H_2O Used in This Study[a]

Hydration Model	Slope of ESPAT-H_2O Linear Fit
Albedo: "small" dark grains[b]	4.2226
Albedo: "large" dark grains[c]	4.0064
Particle size: <45 μm[d]	4.0484
Particle size: 125–250 μm[e]	1.3018

[a]All four models are based on laboratory experiments, and predicted values of H_2O have an accuracy of ~1 wt.% H_2O or better. The observed ESPAT value for each OMEGA observation is multiplied by the slope value below to estimate the water content for each model.

[b]Includes "small" dark grain mixture data from *Milliken and Mustard* [2007a], except clinoptilolite + carbon black mixtures.

[c]Includes all "large" dark grain mixture data from *Milliken and Mustard* [2007a].

[d]Includes data from *Milliken and Mustard* [2005] and *Milliken* [2006, chap. 4].

[e]Based on data for this size fraction of palagonite from *Milliken and Mustard* [2007b].

Murchie et al. [2000] observed similar trends in ISM data for the equatorial regions, though *Calvin* [1997] later used the IBD parameter normalized by the albedo near 2.2 μm to remove this correlation when evaluating Mariner IRS data. However, the spatial coverage of both of these data sets is far less than that presented here, did not cover as wide a range in albedo as the OMEGA data, and did not include observations of the high northern latitudes. Furthermore, laboratory measurements have demonstrated that such albedo correlations result in part from the method [*Milliken and Mustard*, 2007a]; thus we cannot determine the veracity of bright regions being more hydrated than dark regions solely on the basis of these parameters.

3.2. ESPAT Parameter

[25] Our preferred method of estimating absolute H_2O content of the Martian surface is to use the relationship between *Hapke*'s [1993] ESPAT parameter and wt.% H_2O [*Milliken and Mustard*, 2005]. It has been shown that this correlation is linear over a wide range of water contents (~0–15 wt.% H_2O), albedo values (~0.07–0.8), compositions (e.g., clay minerals, hydrated igneous compositions), and provides a much better estimate of absolute water content than band depth, integrated band depth, or apparent absorbance [*Milliken and Mustard*, 2005, 2007a]. The uncertainties in absolute water content as derived from the ESPAT parameter depend primarily on two physical properties of the material being measured: the size of dark particles that give rise to low-albedo spectra and the average particle size of the material being measured. We examined the effects of these properties separately to determine the range in values of absolute water content for Mars, providing what we consider to be the end-member scenarios for the hydration state of the Martian surface.

3.2.1. Comparisons Between Low-Albedo Models

[26] If low-albedo regions on Mars are dark due to the presence of a very fine-grained strong absorber ($\leq$1 μm), similar to the finely-dispersed opaques found in volcanic rocks and carbonaceous chondrites for example, then physical and numerical experiments show that the ESPAT parameter is capable of estimating absolute water content within ~1.6 wt.% H_2O [*Milliken and Mustard*, 2007a]. However, if low-albedo regions merely represent mechanical mixing of bright dust and dark basaltic material (as is likely), then the particle size of the dark component is likely much larger. In these cases, for "large" dark particles, the accuracy of the ESPAT parameter is better than 1 wt.% H_2O. Combining data for physical and numerical observations for low-albedo mixtures with either "large" (>1 μm) or "small" (<1 μm) dark particles yields an accuracy of ~1 wt.% H_2O for a wide range of albedo values and compositions [*Milliken and Mustard*, 2007a]. This suggests that the particle size of the dark component in mixtures containing a strongly absorbing (dark) material is a second order effect on our hydration model relative to the effects of increasing the absorption coefficient [*Milliken and Mustard*, 2007b].

[27] We find that the relative relationships in hydration are qualitatively the same over spatial scales for the "small" or "large" dark grain models: bright and dark regions have similar water contents for equatorial latitudes and there is a distinct increase in hydration with latitude poleward of ~50°N. These trends and values of absolute H_2O content are discussed further below. The mean particle size of the dark material on Mars and whether it behaves spectrally as a fine-grained or coarse-grained darkening agent is somewhat unconstrained, but it is likely that dark regions on Mars are best represented as a mechanical mixture of dark basaltic materials and bright, fine-grained dust. Regardless, the linear relationship between the ESPAT parameter and wt.% H_2O is quite similar for these two scenarios. We find that values of water content estimated from the "large" and "small" dark particle models differ by ~1 wt.% H_2O at most for high latitudes and <0.5 wt.% H_2O for the majority of the Martian surface, values within the uncertainties of this method. On the basis of the similarity of these two models and the uncertainty of the specific particle size for low-albedo materials on Mars, we choose to combine these two possibilities into one model. As stated previously, the combined ESPAT model is capable of estimating water content within ~1 wt.% H_2O given the assumptions used here. The slope of the best fit line that describes the ESPAT-H_2O relationship for each of these two models is presented in Table 1.

3.2.2. Comparisons Between Grain Size Models

[28] The second physical property that will affect our estimates of water content is the particle size of the material being observed. Laboratory data show that the positive slope of the linear relationship between the ESPAT parameter and wt.% H_2O decreases as particle size increases [*Milliken and Mustard*, 2007b]. In this study we compare H_2O contents derived for two possible particle size distributions. The first is based on the results for the combined "small" and "large" low-albedo particle mixtures described above, which includes data for several different hydrous and anhydrous phases, all of which have a particle size <45 μm in diameter (data from *Milliken and Mustard* [2005, 2007a] and *Milliken* [2006]) (Figure 3d). The second scenario is derived from the ESPAT-H_2O relationship observed for laboratory spectra of a palagonite sieved to a size fraction of 125–250 μm (Figure 3e) (data from *Milliken and Mustard* [2007b]). Though the ESPAT parameter is apparently

independent of albedo, we point out that data for the model assuming and effective particle size <45 μm span an albedo range of $\sim$0.07–0.8, whereas the model assuming an effective particle size of 125–250 μm is based on a single palagonite sample with an albedo of $\sim$0.5. As with the two albedo models discussed above, the two particle size models exhibit the same relative trends in water content, though the absolute H_2O values are quite different (Figures 3d and 3e). The difference in estimated H_2O content between the two particle size models is presented in Figure 3f. Equatorial regions commonly differ by <4 wt.% H_2O, though high northern latitudes may differ by as much as 8 wt.% H_2O. Again, we stress that these models only differ in absolute values and each predicts that bright and dark regions in equatorial regions have similar water contents and that hydration increases poleward of $\sim$50°N. Slope values of these ESPAT-H_2O relationships are also presented in Table 1.

[29] Unlike laboratory samples, which are often sieved to a specific range of particle sizes, natural surfaces are often composed of a wide distribution of particle sizes and may be characterized by several distinct modes (i.e., bi-modal or tri-model particle size distributions). Excluding well-sorted deposits such as sand dunes, it is unrealistic to assume that a natural surface will be confined to a specific particle size range such as <45 μm or 125–250 μm. Furthermore, it is important to note that reflectance spectra are not necessarily representative of the mean particle size of a mixture because it is the relative cross-sectional areas of the various components that add linearly to produce an observed spectrum [*Hapke*, 1993]. *Pieters et al.* [1993] demonstrated this by examining lunar soils and concluded that spectra of a planetary regolith would be dominated by the ''finest fraction'' of the particle size distribution. Smaller particles also tend to coat larger grains, thus reducing the probability a photon will interact with the large particles when both are present [*Adams and Filice*, 1967; *Salisbury and Wald*, 1992; *Pieters et al.*, 1993]. In addition to the coating effect of small particles, the presence of surface asperities and rough surface textures also increase the number of scattering interfaces, thus increasing the relative proportion of volume to surface scattering [*Aronson and Emslie*, 1973].

[30] These effects can cause surfaces with a relatively large mean particle size to be more spectrally similar to smaller particles [*Harloff and Arnold*, 2001], as may be the case for low-albedo regions on Mars.

[31] Conversely, bright regions on Mars are dominated by micrometer-sized dust particles that will likely clump together to form aggregates when on the surface, thus having a larger ''effective'' particle size in terms of the spectral signature. Given these complications and the global distribution of bright dust, it is unlikely that spectra of bright regions are representative solely of micrometer-sized dust and that spectra of dark regions are representative solely of particles >125 μm in diameter. Images acquired by the Microscopic Imager on the MER rovers also reveal that the particle size distribution and texture of the Martian surface is quite complex [*Herkenhoff et al.*, 2004, 2006]. Dust storms distribute fine-grained material on a global scale and the surface of Mars, like the Moon, is heavily cratered and undoubtedly contains a large number of particles <125 μm in diameter.

[32] Though we cannot exclude the possibility that some regions of Mars may be dominated numerically by particles >45 μm in diameter, we assume the ''finest fraction'' will dominate reflectance spectra of the surface and consider our model for an effective particle size <45 μm to be a reasonable spectral analog for the Martian surface. We do not attempt to combine these two effective particle size models until more information regarding the particle size distribution of the surface and its effect on reflectance spectra is available; thus we will consider our H_2O contents derived from the 125–250 μm model to represent a lower limit of surface hydration. Future work will focus on placing tighter constraints on this model parameter by including information regarding the particle size distribution of surface materials as derived from other data sets (e.g., thermal inertia derived using TES data) [*Christensen*, 1986; *Christensen and Moore*, 1992; *Mellon et al.*, 2000; *Ruff and Christensen*, 2002; *Putzig et al.*, 2005].

3.3. Global Variations in Water Content

[33] Using our results from the different low-albedo and particle size models examined above, we use the ESPAT model for particles <45 μm in diameter, spanning an albedo range of $\sim$0.07–0.8, and based on data for hydrated clay minerals, zeolites, palagonite, and igneous compositions to provide our best estimates of absolute water content for the surface of Mars. Values derived from this method are compared to values of water-equivalent hydrogen determined by *Feldman et al.* [2004b] in Figure 4. The OMEGA and GRS (neutron) spectrometers sample extremely different depths, with the former being on the order of 10–100 s of micrometers and the latter on the order of $\sim$1 m. Remarkably, both instruments exhibit similar trends with latitude in the northern hemisphere. Estimates of water content derived from OMEGA data range from $\sim$2–5 wt.% H_2O for equatorial latitudes ($\sim$0–45°N; Figure 4a), similar to the WEH values of *Feldman et al.* [2004b] (Figure 4b). Similarly, water contents derived from both data sets exhibit an increase in hydration poleward of $\sim$45–60°N, though the OMEGA data yield values from $\sim$5–15 wt.% H_2O, whereas WEH values are up to 5 times higher than this. *Pimentel et al.* [1974] observed a similar increase in hydration with latitude using Mariner 6 and 7 IRS data. The discrepancy in absolute H_2O values between OMEGA and GRS is partially a result of the different viewing depths of the two instruments (the GRS instrument suite is capable of detecting water-ice buried at depth) as well as the model used to estimate WEH, which assumes a ''dry'' upper layer of 2 wt.% H_2O. Regardless, the similar results of these two studies suggests that the water content of the uppermost fraction of the regolith at these high latitudes is likely controlled by both water ice buried at depth and the concentration of water vapor in the overlying atmosphere (relative humidity). The uppermost portion of the regolith will seek equilibrium with these under and overlying reservoirs of H_2O.

[34] There are two areas of noticeable disagreement between surface hydration as seen by OMEGA and WEH values for the upper 1 m of regolith as seen by the Neutron Spectrometer. The first is a region including Acidalia

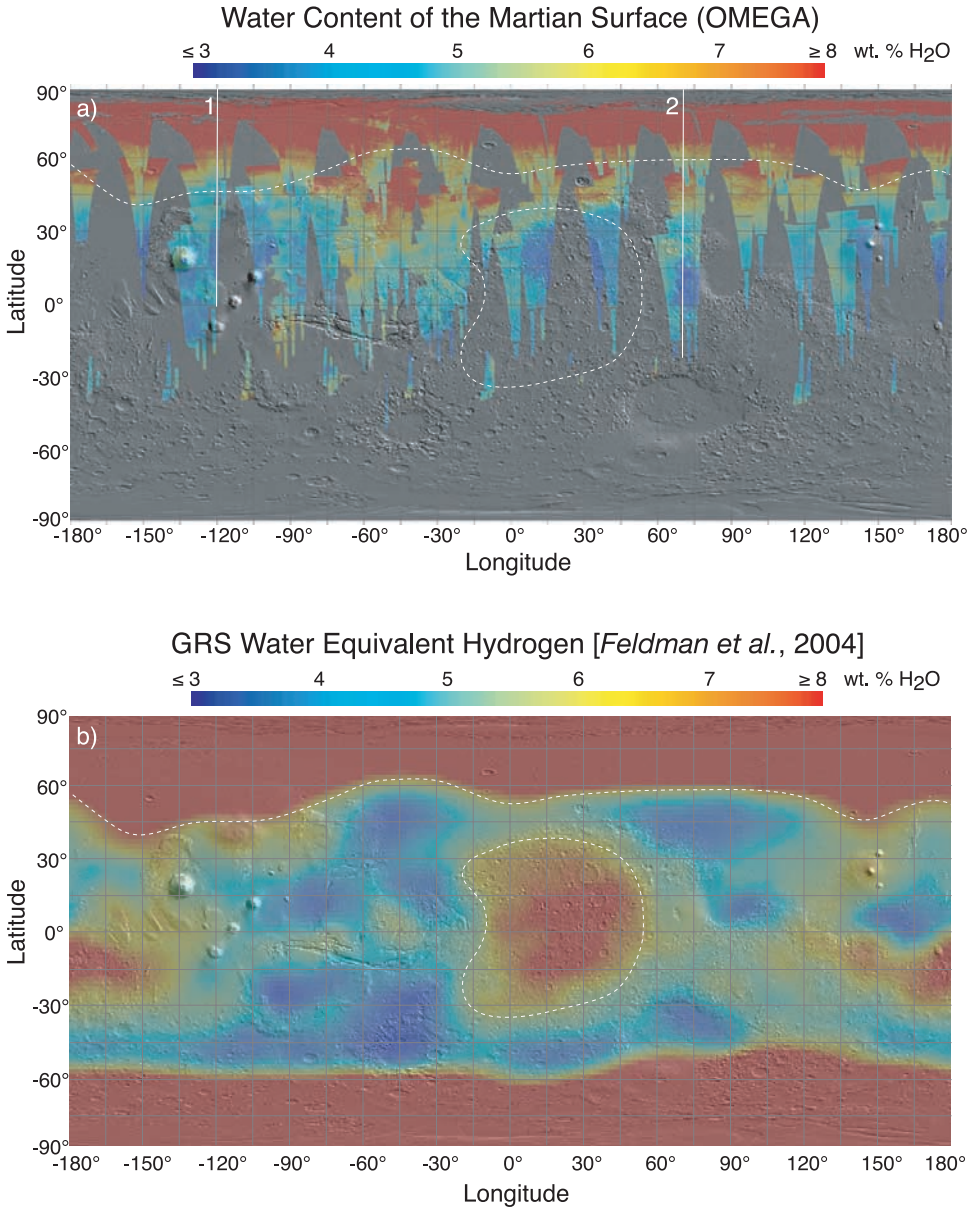

Figure 4. Maps of (a) our ideal model for estimating water content, assuming an effective particle size <45 μm and that albedo variations are caused by the presence of either large or small dark grains, and (b) water equivalent hydrogen as estimated by *Feldman et al.* [2004b] from Mars Odyssey Neutron Spectrometer data. Dashed white lines outline the regions of increased WEH in Arabia Terra (circle in equatorial zone) and high latitudes for comparison to our results in Figure 4a. Both instruments detect an increase in hydration at high northern latitudes, but OMEGA data do not suggest an increase in equatorial regions (Arabia Terra). Vertical white lines in Figure 4a depict locations of latitude profiles presented in Figure 5.

Planitia (approximately 0–60°E, 0–45°N), which has a water content of ~5–7 wt.% H_2O as estimated from the OMEGA data, an increase of ~1–3 wt.% H_2O relative to surrounding areas of similar latitude. Values of WEH for this region, however, are on the order of 2–5 wt.% and are among the lowest for the equatorial regions. The second area of discrepancy between these two estimates of hydration is the high-albedo, dusty region of Arabia Terra. Estimates of WEH for this region approach ~10 wt.% H_2O (Figure 4b), whereas our model and the OMEGA data show no increase in water content for this region relative to its surroundings. The OMEGA coverage presented here for this area is incomplete, but an examination of other orbits in this region which are not in the "nominal" calibration state also suggest Arabia Terra has a relatively low water content at the surface. Again, discrepancies between these two data sets may be attributed to the different sensing depths of the instruments as well as the models used to estimate wt.% H_2O. However, the quantitative agreement for most equatorial regions and the qualitative agreement at high latitudes

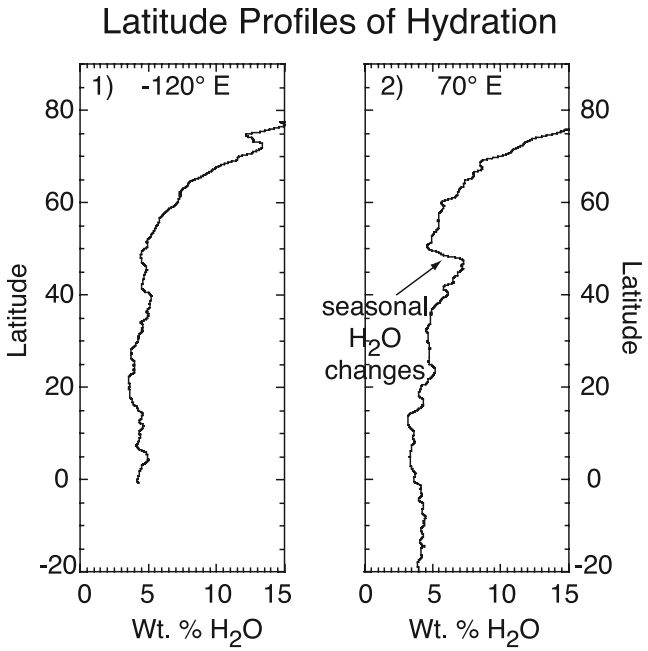

Figure 5. Latitude profiles of hydration corresponding to the vertical white lines (labeled 1 and 2) in Figure 4a. OMEGA orbits for profile 1 were acquired during northern spring and exhibit an increase in hydration poleward of ~45°N. Profile 2 contains data acquired during northern spring and summer and shows that hydration increases with latitude, revealing a change of ~2–3 wt.% H_2O near latitudes of ~40–45°N, corresponding to a seasonal decrease in surface hydration during the transition from northern spring to northern summer [*Jouglet et al.*, 2007].

suggest that both methods are valid and are revealing complex variations in hydration with depth.

4. Discussion

[35] Unlike band depth, integrated band depth, and apparent absorbance values, the estimates of H_2O content derived from the ESPAT parameter do not exhibit a strong positive correlation to albedo. Bright and dark regions in equatorial latitudes have similar water contents, in the range of 2–5 wt.% H_2O, whereas bright and dark regions at high latitudes contain ~5–15 wt.% H_2O (Figure 4a). Our hydration estimates for the equatorial regions and the Viking lander sites are 2–3 times greater than as measured by the GCMS instrument on the Viking landers (1–2 wt.% H_2O), but these instruments were not designed to accurately measure the water content of the soil and may be off by a factor of five at most [*Biemann et al.*, 1977]. However, the question still remains: what is the form of this H_2O observed on the Martian surface?

[36] For this discussion we will divide H_2O into two types, based on its ability to respond to changes in relative humidity: adsorbed water and bound structural water. Adsorbed water can be further divided into two types that include H_2O adsorbed onto grain surfaces (surface adsorbed H_2O) as well as H_2O that is easily removed or added to a mineral via changing the relative humidity. The latter may include water stored in the interlayer region of smectites, the channel structures of zeolites, or hydrated sulfates that can vary in water content under current Mars conditions, such as $MgSO_4 \cdot nH_2O$ [*Vaniman et al.*, 2004]. We will refer to this form of water as structurally adsorbed H_2O. Structurally bound water will refer to H_2O that is not readily exchanged between the hydrated phase and the atmosphere on short timescales (i.e., stable during seasonal cycles). This form of water requires an input of energy, such as through heating, to be removed from the host material. Examples may include, but are not limited to, hydrated glass, hydrated Fe-oxides, and some H_2O in palagonite [*Milliken and Mustard*, 2005]. All three forms of water are likely present on Mars, though the relative amounts of each may vary spatially and temporally.

[37] Some portion of the observed water content may be surface adsorbed H_2O that is present on all particles, independent of composition. However, experimental work by *Zent and Quinn* [1995, 1997] suggests the amount of water in this form is likely <1 wt.% H_2O under current Mars conditions. This value is much too low to account for all of the hydration we observe at equatorial and high latitudes; therefore much of the water in these regions must be structurally adsorbed or structurally bound water associated with hydrated minerals or amorphous phases. Unfortunately, the composition of such hydrated phase(s) is not evident from the OMEGA spectra for most of the surface, which only exhibit an increase in the 3 μm region with no corresponding absorptions indicative of sulfates or phyllosilicates as are found in localized regions on Mars [*Bibring et al.*, 2005; *Gendrin et al.*, 2005; *Langevin et al.*, 2005; *Poulet et al.*, 2005].

[38] It is clear from Figure 4a that overlapping observations at high latitudes exhibit different water contents. Some observations exhibit water contents upwards of ~8 wt.% H_2O at latitudes >45°N, whereas overlapping observations exhibit values <7 wt.% H_2O at these same locations. The former correspond to data acquired during northern spring and the latter to data acquired during northern summer. *Jouglet et al.* [2007] have shown that these changes in hydration are not an effect of surface frost or instrumental artifacts, but rather a result of the exchange of water vapor between the regolith and atmosphere. Atmospheric and ice-stability models also predict that the exchange of water vapor between these two reservoirs has played an important role in the recent history of Mars [*Forget et al.*, 2006; *Mellon et al.*, 2004; *Mischna et al.*, 2003; *Mellon and Jakosky*, 1995], though direct quantitative measurements of H_2O-exchange have not yet been available to fully constrain these studies. Our estimates of absolute water content suggest as much as 2–4 wt.% H_2O is exchanged between the regolith and atmosphere at latitudes >45°N during the transition from northern spring to northern summer. This decrease in hydration occurs at all longitudes, as evident from Figure 4a and the latitude hydration profiles presented in Figure 5 and are discussed in detail by *Jouglet et al.* [2007].

[39] *Ruff* [2004] suggested zeolites may be a minor constituent of the Martian dust. Therefore it is possible that minerals which readily exchange H_2O, such as clays, sulfates, or zeolites, are present in the soil at high latitudes but in concentrations that are below their detection limit by

OMEGA, such that only the effects of their strong fundamental hydration features at 3 μm are observed and not overtone H_2O or metal-OH^- absorptions near 1.9 and 2.2–2.4 μm. Unfortunately, only the presence and not the absence of absorption features can be used to infer mineralogy; therefore the composition of hydrated phase(s) at high latitudes cannot be determined from current observations. However, the estimates of H_2O from this study and the changes in hydration with season described by *Jouglet et al.* [2007] imply that the hydrated phase(s) must be capable of (1) holding large amounts of water (5–15 wt.%) and (2) exchanging at least 2–4 wt.% of that water with the atmosphere on seasonal timescales.

[40] As mentioned previously, values of WEH derived by *Feldman et al.* [2004b] were based on a two-layer model that assumed an upper "dry" layer of unknown thickness with a water content of 2 wt.%. Recent attempts to estimate WEH at high latitudes have focused on using count rates of thermal as well as fast and epithermal neutrons, but these results suggest the Neutron Spectrometer data cannot be fit with a two-layer model in which the upper layer has more than ~5 wt.% H_2O (W. Feldman, personal communication, 2006). This apparent contradiction of our hydration estimates is simply a result of the extreme differences in sensing depths between the OMEGA and GRS instruments. Furthermore, it highlights the over-simplification of assuming a two-layer model. We suggest that the hydration gradient with depth is more complex than this and is perhaps described better by a three-layer model than a two-layer model. In this scenario, the upper layer would be constrained by estimates of the thickness of porous regolith that exchanges water vapor with the atmosphere on seasonal cycles and an estimate of water content determined by our results using OMEGA data (i.e., Figure 4a). The thickness and water content of the underlying layer (the new "dry" layer) and the water (ice) content of the bottom, semi-infinite layer could then be determined from the NS counting rates.

[41] The GRS and NS results predict a shallow ice reservoir at high northern latitudes; therefore it is not unreasonable to assume that the soil above these areas would exhibit an increase in water content relative to soil over ice-free regions in the lower latitudes. The hydration state of the uppermost fraction of the surface, in fact, will seek equilibrium between the water ice buried at depth and the water vapor in the overlying atmosphere. A three-layer model may also be an over-simplification of the true gradient in hydration with depth, but it is clear from Figure 4a that the hydration state of the Martian surface is spatially quite variable and often greater than 2 wt.% H_2O, which is not accurately accounted for by a simple two-layer model.

[42] *Fialips et al.* [2005], *Vaniman et al.* [2004], and *Bish et al.* [2003] showed that clay minerals, zeolites, and sulfates are capable of holding variable amounts of water under current Mars pressure and temperature conditions. These minerals may account for the increased signature of WEH in equatorial regions such as Arabia Terra (Figure 4b) [*Feldman et al.* 2004a; *Fialips et al.*, 2005]. We do not observe an increase in surface hydration for this bright region, though the Neutron Spectrometer is sensitive to a much greater depth than OMEGA. Arabia is a bright, dusty region of low thermal inertia [*Mellon et al.*, 2000; *Putzig et al.*, 2005] and it is plausible that hydrated minerals are present beneath a centimeters-thick dust cover, thus obscuring them from the shallow penetration depth of OMEGA. Small exposures of layered materials inside craters within this region, however, appear "warm" in THEMIS night IR images relative to surrounding terrains and exhibit increased hydration values of ~5–7 wt.% H_2O. These observations support the hypothesis that spatially extensive deposits of hydrated minerals may exist within Arabia. OMEGA is capable of detecting these deposits only when the dust cover is minimal or absent, commonly in craters, thereby providing a window into the layered, hydrated subsurface.

[43] Local outcrops of increased hydration in Arabia, similar to hydrated regions at high latitudes, exhibit only an increase in the strength of the 3 μm band and lack other diagnostic absorptions between 1.8–2.5 μm indicative of specific mineral assemblages. This is in contrast to other areas of increased hydration surrounding Arabia, including Terra Meridiani, Aram Chaos, Mawrth Vallis, and Nili Fossae/Syrtis Major to name a few. *Poulet et al.* [2005] identified hydrated phyllosilicates in Mawrth Vallis and Nili Fossae on the basis of the presence of absorptions centered near 1.9 μm (combination overtone of the H_2O bend + stretch) and 2.2–2.3 μm (metal-OH stretch) in spectra for these regions. We estimate these regions to have ~7–9 wt.% H_2O, an increase of ~2–4 wt.% H_2O relative to surrounding areas (Figure 6). *Gendrin et al.* [2005] described the presence of hydrated sulfates in equatorial regions, including deposits in Valles Marineris, Aram Chaos, Terra Meridiani, and Juventae Chasma. These regions commonly exhibit hydration values of 5–7 wt.% H_2O, an increase of ~1–3 wt.% H_2O relative to surrounding regions. An increase in hydration for such regions is consistent with the observations of *Baldridge and Calvin* [2004], who detected an increase in the normalized integrated band depth parameter for Aram Chaos and Terra Meridiani using Mariner 6 and 7 IRS data. *Jouglet et al.* [2007] have shown that these phyllosilicate and sulfate-rich regions exhibit an increase in the strength of the both the 1.9 and 3 μm hydration absorptions, confirming that they are unique in composition and hydration state when compared to surrounding terrains.

[44] We conclude this discussion by noting that it may be possible to combine our results with thermodynamic predictions of the hydration states of minerals to estimate the relative proportions of hydrated phases and dust in these regions, assuming the composition and spectra of these surfaces are dominated by these two phases. If the phyllosilicates in Mawrth Vallis are identified as nontronite [*Poulet et al.*, 2005], for instance, then experimental data estimating the amount of water these minerals can store under current Mars pressure and temperature conditions [*Bish et al.*, 2003; *Fialips et al.*, 2005] can be used to determine the relative proportions of dust and nontronite that are required to fit our estimated values of wt.% H_2O.

[45] The hydrated sulfates and phyllosilicates observed to date occur primarily in Noachian-aged crust. This age relationship and the large hydration signature in Arabia Terra suggest that water-rock interactions and aqueous alteration of basaltic material to form hydrated minerals may have been spatially extensive in the early history of Mars [*Bibring et al.*, 2006]. Understanding the volumetric

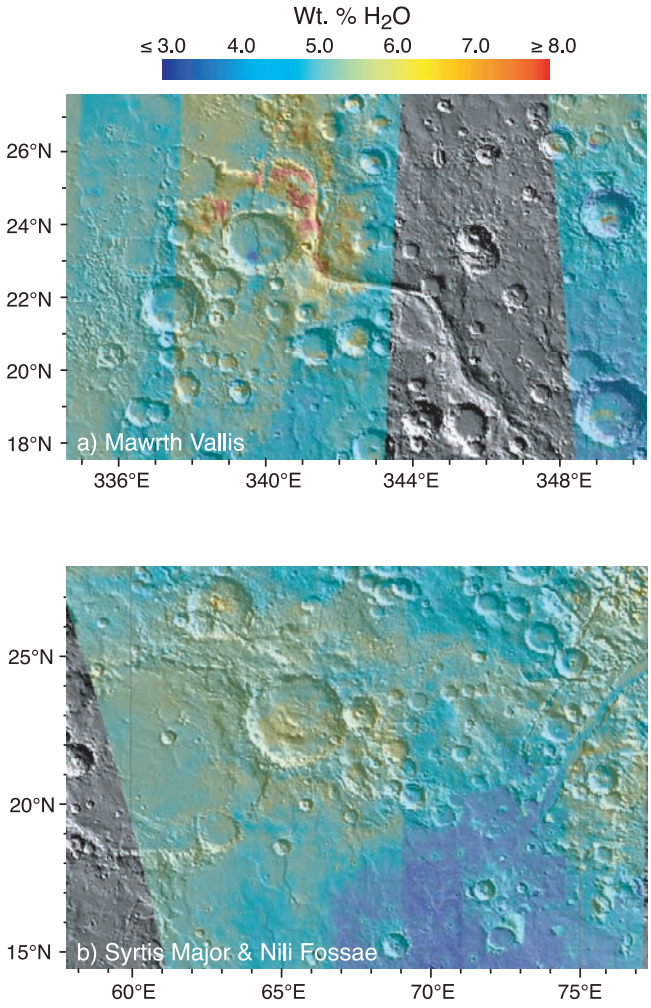

Figure 6. Hydration maps for regions with phyllosilicates, including (a) the Mawrth Vallis region (centered near 22.5°N, 343°E) and (b) the Nili Fossae-Syrtis Major region (centered near 21°N, 68°E). These regions exhibit water contents 2–3 times higher than surrounding terrains with similar albedo values, approaching values of 6–9 wt.% H_2O.

abundances of these hydrated phases may help to constrain the duration and rate of this alteration. Therefore, in addition to providing an estimate of surface hydration that is independent of the Viking and GRS measurements, the 3 μm band observed in all OMEGA spectra has the potential to provide information about the abundance, distribution, and formation of hydrated minerals on the surface of Mars.

5. Conclusions

[46] All visible-near infrared reflectance spectra of the surface of Mars acquired by the Mars Express OMEGA spectrometer exhibit a strong 3 μm hydration absorption attributed to water adsorbed on grain surfaces and/or adsorbed and bound in hydrous minerals. We have compared integrated band depth, apparent absorbance, and effective single-particle absorption-thickness parameter values for the 3 μm absorption observed in spectra acquired while the OMEGA instrument was responding in the nominal calibration state. Integrated band depth and apparent absorbance values exhibit a positive correlation to albedo when derived from reflectance spectra, giving the impression that bright regions are potentially more hydrated than dark regions. Physical and numerical experiments suggest this correlation is in part a result of the method, for which absorptions in low-albedo materials are strongly affected by non-linear compression effects. This bias makes an estimate of H_2O content from these values impractical, though values for both parameters exhibit an increase for high northern latitudes that is not correlated solely to albedo.

[47] Estimates of wt.% H_2O derived from ESPAT values for the different low-albedo and particle size models examined here all suggest that bright and dark regions in the equatorial latitudes have similar water contents, whereas hydration increases with latitude poleward of ~50°N. Absolute values of wt.% H_2O are less dependent on whether albedo differences are caused by the presence of large or small dark grains and more dependent on the "effective" particle size of the area being measured. If the surface of Mars is dominated spectrally by particles 125–250 μm in diameter, then equatorial regions have ~1–2 wt.% H_2O and high northern latitudes increase to ~2–5 wt.% H_2O, likely a lower limit of surface hydration. If spectra of the surface are dominated by smaller particles (<45 μm in diameter), as expected for a planetary regolith, then the near-surface in equatorial regions holds ~2–5 wt.% H_2O and high northern latitudes store 5–15 wt.% H_2O. However, we cannot exclude that dark regions may be somewhat less hydrated than bright regions if their spectra are dominated by "large" particles and those of bright regions by "small" particles. This possibility can be explored further once we obtain additional information regarding spatial variations in the particle size distribution of the Martian surface.

[48] Values of water content for overlapping observations at mid to high northern latitudes suggest as much as 2–4 wt.% H_2O is exchanged between the regolith and atmosphere at all longitudes during the transition from northern spring to northern summer. Latitudes poleward of ~45° store upwards of 8 wt.% H_2O during northern spring, whereas this boundary shifts to a latitude of ~60°N during northern summer. The latter agrees qualitatively with estimates of water-equivalent hydrogen as modeled using CO_2 frost-free Mars Odyssey Neutron Spectrometer data. Estimates of WEH are constrained by a two-layer model that commonly assumes a "dry" upper layer of 2 wt.% H_2O. Our data suggest the surface is significantly more hydrated than this at high northern latitudes; thus a three-layer model may be more appropriate.

[49] Unlike estimates of WEH, estimates of wt.% H_2O derived from OMEGA data do not exhibit an increase in hydration over Arabia Terra, likely a result of a centimeters-thick dust cover obscuring hydrated phases from the view of OMEGA. Areas of sulfate-rich material exhibit an increase in hydration relative to surrounding terrains, up to ~5–7 wt.% H_2O, whereas phyllosilicate-rich areas exhibit the highest water contents within the equatorial latitudes, up to 7–9 wt.% H_2O. The ESPAT model has an accuracy of ~1 wt.% H_2O using the assumptions presented here, but laboratory experiments suggest additional information regarding the composition and particle size of hydrated

phases on Mars can help to improve this to 0.5 wt.% H_2O or better. We have combined this model with OMEGA data to produce the first quantitative, high-resolution map of water content within the uppermost fraction of the Martian surface. These results will aid in improving atmospheric and climate models, selecting landing sites for future missions, and help to provide a better understanding of the past and present role of water and aqueous alteration on Mars.

References

Adams, J. B., and A. L. Filice (1967), Spectral reflectance 0.4 to 2.0 microns of silicate rock powders, *J. Geophys. Res.*, *72*, 5705–5715.

Anderson, D. M., and A. R. Tice (1979), The analysis of water in the Martian regolith, *J. Mol. Evol.*, *14*, 33–38.

Aronson, J. R., and A. G. Emslie (1973), Spectral reflectance and emittance of particulate materials 2: Application and results, *Appl. Opt.*, *12*, 2573–2584.

Baldridge, A. M., and W. M. Calvin (2004), Hydration state of the Martian coarse-grained hematite exposures: Implications for their origin and evolution, *J. Geophys. Res.*, *109*, E04S90, doi:10.1029/2003JE002066.

Bandfield, J. L., and M. D. Smith (2003), Multiple emission angle surface-atmosphere separations of Thermal Emission Spectrometer data, *Icarus*, *161*, 47–65.

Bibring, J.-P., et al. (1989), Results from the ISM experiment, *Nature*, *341*, 591–593.

Bibring, J.-P., et al. (2004), OMEGA: Observatoire pour la Minéralogie, l'Eau, les Glaces et l'Activité, in *Mars Express: The Scientific Payload*, edited by A. Wilson, *Eur. Space Agency Spec. Publ.*, *ESA-1240*, 37–49.

Bibring, J.-P., et al. (2005), Mars surface diversity as revealed by the OMEGA/Mars Express observations, *Science*, *307*, 1576–1581.

Bibring, J.-P., et al. (2006), Global mineralogical and aqueous Mars history derived from OMEGA/Mars Express data, *Science*, *312*, 400–404.

Biemann, K., J. Oro, P. Toulmin, L. E. Orgel, A. O. Nier, D. M. Anderson, D. Flory, A. V. Diaz, D. R. Rushneck, and P. G. Simmonds (1977), The search for organic substances and inorganic volatile compounds in the surface of Mars, *J. Geophys. Res.*, *82*, 4641–4658.

Bish, D. L., J. W. Carey, D. T. Vaniman, and S. J. Chipera (2003), Stability of hydrous minerals on the Martian surface, *Icarus*, *164*, 96–103.

Boynton, W. V., et al. (2002), Distribution of hydrogen in the near surface of Mars: Evidence for subsurface ice deposits, *Science*, *297*, 81–85.

Calvin, W. M. (1997), Variation of the 3 μm absorption feature on Mars: Observations over eastern Valles Marineris by the Mariner 6 infrared spectrometer, *J. Geophys. Res.*, *102*, 9097–9107.

Christensen, P. R. (1986), Regional dust deposits on Mars: Physical properties, age, and history, *J. Geophys. Res.*, *91*, 3533–3545.

Christensen, P. R., and H. J. Moore (1992), The Martian surface layer, in *Mars*, edited by H. H. Kieffer et al., pp. 686–729, Univ. of Ariz. Press, Tucson.

Christensen, P. R., et al. (2004), Mineralogy at Meridiani Planum from the Mini-TES experiment on the Opportunity Rover, *Science*, *306*, 1733–1739.

Clark, R. N. (1983), Spectral properties of mixtures of montmorillonite and dark carbon grains: Implications for remote sensing minerals containing chemically and physically adsorbed water, *J. Geophys. Res.*, *88*, 10,635–10,644.

Clark, R. N., and T. L. Roush (1984), Reflectance spectroscopy: Quantitative analysis techniques for remote sensing applications, *J. Geophys. Res.*, *89*, 6329–6340.

Erard, S., and W. Calvin (1997), New composite spectra of Mars, 0.4–5.7 μm, *Icarus*, *130*, 449–460.

Feldman, W. C., et al. (2002), Global distribution of neutrons from Mars: Results from Mars Odyssey, *Science*, *297*, 75–78.

Feldman, W. C., et al. (2004a), Hydrated states of $MgSO_4$ at equatorial latitudes on Mars, *Geophys. Res. Lett.*, *31*, L16702, doi:10.1029/2004GL020181.

Feldman, W. C., et al. (2004b), Global distribution of near-surface hydrogen on Mars, *J. Geophys. Res.*, *109*, E09006, doi:10.1029/2003JE002160.

Fialips, C. I., J. W. Carey, and D. L. Bish (2005), Hydration-dehydration behavior and thermodynamics of chabazite, *Geochim. Cosmochim. Acta*, *69*, 2293–2308.

Forget, F., R. M. Haberle, F. Montmessin, B. Levrard, and J. W. Head (2006), Formation of glaciers on Mars by atmospheric precipitation at high obliquity, *Science*, *311*, 368–371.

Gendrin, A., et al. (2005), Sulfates in Martian layered terrains: The OMEGA/Mars Express view, *Science*, *307*, 1587–1591.

Grotzinger, J., et al. (2005), Stratigraphy and sedimentology of a dry to wet eolian depositional system, Burns formation, Meridiani Planum, Mars, *Earth Planet. Sci. Lett.*, *240*, 11–72.

Hapke, B. W. (1993), *Theory of Reflectance and Emittance Spectroscopy*, 455 pp., Cambridge Univ. Press, Cambridge, U. K.

Harloff, J., and G. Arnold (2001), Near-infrared reflectance spectroscopy of bulk analog materials for planetary crust, *Planetary Space Sci.*, *49*, 191–211.

Herkenhoff, K. E., et al. (2004), Textures of the soils and rocks at Gusev Crater from Spirit's Microscopic Imager, *Science*, *305*, 824–826.

Herkenhoff, K. E., et al. (2006), Overview of the Microscopic Imager Investigation during Spirit's first 450 sols in Gusev crater, *J. Geophys. Res.*, *111*, E02S04, doi:10.1029/2005JE002574.

Houck, J. R., J. B. Pollack, C. Sagan, D. Schaack, and J. A. Decker Jr. (1973), High altitude infrared spectroscopic evidence for bound water on Mars, *Icarus*, *18*, 470–480.

Jouglet, D., F. Poulet, J. Mustard, R. Milliken, J.-P. Bibring, Y. Langevin, and B. Gondet (2007), Hydration state of the Martian surface as seen by Mars Express OMEGA: 1. Analysis of the 3 μm hydration feature, *J. Geophys. Res.*, *112*, E08S06, doi:10.1029/2006JE002846.

Kortum, G. (1969), *Reflectance Spectroscopy*, 366 pp., Springer, New York.

Kuzmin, R. O., P. R. Christensen, and M. Zolotov (2004), Global mapping of Martian bound water at 6.1 microns based on TES data: Seasonal hydration-dehydration of surface minerals, *Proc. Lunar Planet. Sci. Conf. 35th*, Abstract 1810.

Langevin, Y., F. Poulet, J.-P. Bibring, and B. Gondet (2005), Sulfates in the north polar region of Mars detected by OMEGA/Mars Express, *Science*, *307*, 1584–1586.

Mellon, M. T., and B. M. Jakosky (1995), The distribution and behavior of Martian ground ice during past and present epochs, *J. Geophys. Res.*, *100*, 11,781–11,799.

Mellon, M. T., B. M. Jakosky, H. H. Kieffer, and P. R. Christensen (2000), High-resolution thermal inertia mapping from the Mars Global Surveyor Thermal Emission Spectrometer, *Icarus*, *148*, 437–455.

Mellon, M. T., W. C. Feldman, and T. H. Prettyman (2004), The presence and stability of ground ice in the southern hemisphere of Mars, *Icarus*, *169*, 324–340.

Milliken, R. E. (2006), Estimating the water content of geologic materials using near-infrared reflectance spectroscopy: Applications to laboratory and spacecraft data, Ph.D. dissertation, 404 pp., Brown Univ., Providence.

Milliken, R. E., and J. F. Mustard (2005), Quantifying absolute water content of minerals using near-infrared reflectance spectroscopy, *J. Geophys. Res.*, *110*, E12001, doi:10.1029/2005JE002534.

Milliken, R. E., and J. F. Mustard (2007a), Estimating the water content of hydrated minerals using reflectance spectroscopy I: Effects of darkening agents and low-albedo materials, *Icarus*, *189*, 550–573.

Milliken, R. E., and J. F. Mustard (2007b), Estimating the water content of hydrated minerals using reflectance spectroscopy II: Effects of particle size, *Icarus*, *189*, 574–588.

Mischna, M. A., M. I. Richardson, R. J. Wilson, and D. J. McCleese (2003), On the orbital forcing of Martian water and CO_2 cycles: A general circulation model study with simplified volatile schemes, *J. Geophys. Res.*, *108*(E6), 5062, doi:10.1029/2003JE002051.

Mitrofanov, I., et al. (2002), Maps of subsurface hydrogen from the High Energy Neutron Detector, Mars Odyssey, *Science*, *297*, 78–81.

Murchie, S., J. Mustard, J. Bishop, J. W. Head, C. Pieters, and S. Erard (1993), Spatial variations in the spectral properties of bright regions on Mars, *Icarus*, *105*, 454–468.

Murchie, S., L. Kirkland, S. Erard, J. Mustard, and M. Robinson (2000), Near-infrared spectral variations of Martian surface materials from ISM imaging spectrometer data, *Icarus*, *147*, 444–471.

Mustard, J. F., and C. M. Pieters (1989), Photometric phase functions of common geologic minerals and applications to quantitative analysis of mineral mixture reflectance spectra, *J. Geophys. Res.*, *94*, 13,619–13,634.

Mustard, J. F., F. Poulet, A. Gendrin, J.-P. Bibring, Y. Langevin, B. Gondet, N. Mangold, G. Bellucci, and F. Altieri (2005), Olivine and pyroxene diversity in the crust of Mars, *Science*, *307*, 1594–1597.

Piatek, J. L., B. W. Hapke, R. M. Nelson, W. D. Smythe, and A. Snyder Hale (2004), Scattering properties of planetary regolith analogs, *Icarus*, *171*, 531–545.

Pieters, C. M., E. M. Fischer, O. Rode, and A. Basu (1993), Optical effects of space weathering: The role of the finest fraction, *J. Geophys. Res.*, *98*, 20,817–20,824.

Pimentel, G. C., P. B. Forney, and K. C. Herr (1974), Evidence about hydrate and solid water in the Martian surface from the 1969 Mariner Infrared Spectrometer, *J. Geophys. Res.*, *79*, 1623–1634.

Poulet, F., J. P. Bibring, J. F. Mustard, A. Gendrin, N. Mangold, Y. Langevin, R. E. Arvidson, B. Gondet, and C. Gomez (2005), Phyllosilicates on Mars and implications for early Martian climate, *Nature*, *438*, 623–627.

Putzig, N. E., M. T. Mellon, K. A. Kretke, and R. E. Arvidson (2005), Global thermal inertia and surface properties of Mars from the MGS mapping mission, *Icarus*, *173*, 325–341.

Ruff, S. W. (2004), Spectral evidence for zeolite in the dust on Mars, *Icarus*, *168*, 131–143.

Ruff, S. W., and P. R. Christensen (2002), Bright and dark regions on Mars: Particle size and mineralogical characteristics based on Thermal Emission Spectrometer data, *J. Geophys. Res.*, *107*(E12), 5127, doi:10.1029/2001JE001580.

Salisbury, J. W., and A. D. Wald (1992), The role of volume scattering in reducing spectral contrast of reststrahlen bands in spectra of powdered minerals, *Icarus*, *96*, 121–128.

Sinton, W. M. (1967), On the composition of Martian surface materials, *Icarus*, *6*, 222–228.

Squyres, S. W., and A. H. Knoll (2005), Sedimentary rocks at Meridiani Planum: Origin, diagenesis, and implications for life on Mars, *Earth Planet. Sci. Lett.*, *240*, 1–10.

Squyres, S. W., et al. (2004), In situ evidence for an ancient aqueous environment at Meridiani Planum, Mars, *Science*, *306*, 1709–1714.

Vaniman, D. T., D. L. Bish, S. J. Chipera, C. I. Fialips, J. W. Carey, and W. C. Feldman (2004), Magnesium sulphate salts and the history of water on Mars, *Nature*, *431*, 663–665.

Yen, A. S., B. C. Murray, and G. R. Rossman (1998), Water content of the Martian soil: Laboratory simulations of reflectance spectra, *J. Geophys. Res.*, *103*, 11,125–11,134.

Zent, A. P., and R. C. Quinn (1995), Simultaneous adsorption of CO_2 and H_2O under Mars-like conditions and application to the evolution of the Martian climate, *J. Geophys. Res.*, *100*(E3), 5341–5349.

Zent, A. P., and R. C. Quinn (1997), Measurement of H_2O adsorption under Mars-like conditions: Effects of adsorbent heterogeneity, *J. Geophys. Res.*, *102*(E4), 9085–9095.

J.-P. Bibring, B. Gondet, D. Jouglet, Y. Langevin, and F. Poulet, Institut d'Astrophysique Spatiale (IAS), Bâtiment 121, F-91405 Orsay Cedex, France.

R. E. Milliken, Jet Propulsion Laboratory, California Institute of Technology, 4800 Oak Grove Drive, Pasadena, CA 91109, USA. (ralph.milliken@jpl.nasa.gov)

J. F. Mustard, Department of Geological Sciences, Brown University, Providence, RI 02912, USA.